ACS APPLIED MATERIALS & INTERFACES

Research Article

www.acsami.org

Synthesis of Monodisperse, Hierarchically Mesoporous, Silica Microspheres Embedded with Magnetic Nanoparticles

Yong Wang,[†] Jie He,[†] Jiwei Chen,[†] Lianbing Ren,[†] Biwang Jiang,*[,†] and Jing Zhao*[,†,‡]

[†]Nano-Micro Materials Research Center, School of Chemical Biology & Biotechnology, Peking University Shenzhen Graduate School, Shenzhen 518055, China.

[‡]State Key Laboratory of Pharmaceutical Biotechnology, School of Life Sciences, Nanjing University, Nanjing 210093, China.

ABSTRACT: We report a preparation method for the synthesis of monodisperse magnetic polymer/silica hybrid microspheres using polymer microspheres incorporated with magnetic nanoparticles as a novel template. Monodisperse, hierarchically mesoporous, silica microspheres embedded with magnetic nanoparticles were successfully fabricated after the calcination of the hybrid microspheres. The magnetic nanoparticles were encapsulated in silica and distributed over the whole area of the porous microspheres without leakage. The resulting inorganic materials possess highly useful properties such as high magnetic nanoparticle loading, high surface area, and large pore volumes. The hierarchically mesoporous magnetic silica microspheres resulted in a high bovine serum albumin (BSA) protein adsorption capacity (260 mg/g) and a fast adsorption rate (reaching equilibrium with 8 h).

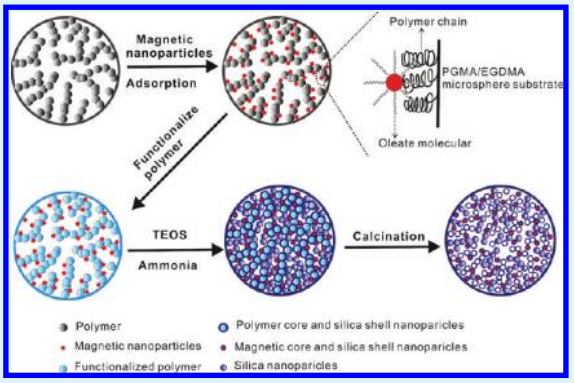

KEYWORDS: *hierarchical pores, magnetic nanoparticles, mesoporous silica, microspheres, protein adsorption*

INTRODUCTION

Magnetic mesoporous silica microspheres exhibit interesting physical and chemical properties, such as large surface areas, magnetic properties, low toxicity, and chemical modifiable surfaces, leading to attractive applications in magnetic bioseparation,[1] heterogeneous catalysis,[2] enzyme immobilization,[3] targeted drug delivery,[4] and water treatment adsorbents.[5,6] Therefore, significant efforts have been devoted to making magnetic silica microspheres with controlled pore structure, particle size, and morphologies. For example, core/shell type magnetic mesoporous silica nanocomposites can be synthesized by a combination of surfactant-based self-assembly and sol−gel process.[7−10] Recently, yolk/shell mesoporous structures have been reported by a few groups based on etching approach,[11] microemulsion method[12] and vesicle template.[13] By using cetytrimethylammonium bromide (CTAB) surfactant as a structure agent for transferring the magnetic particles from oil to water, magnetic nanoparticles have been successfully encapsulated into the mesoporous silica nanospheres.[14−17] The diameters of the above-mentioned magnetic silica microspheres are usually in the range of hundreds of nanometers. The pore structures of these magnetic silica particles are monomodal small mesopores without interconnecting large mesopores, rendering them ineffective carriers for simultaneous loading of different species with varied sizes. Thus, it is highly desirable to develop a simple preparation of hierarchical mesoporous magnetic microspheres. Especially attractive are micrometer-sized microspheres, which could be applied in enrichment and biological separation because of their faster reaction kinetics due to their suspension in homogeneous solution and the associated advantages in diffusion rates. To the best of our knowledge, such microspheres have not been reported.

Herein, we demonstrate an effective method for the synthesis of highly monodisperse magnetic mesoporous silica microspheres embedded with magnetic nanoparticles using a templating approach. The obtained microspheres are highly monodisperse micrometer-sized microspheres, possessing high magnetic nanoparticle loading (10.3%), hierarchically interconnecting mesoporous structure (3.8, 13.2, and 44.7 nm), high surface area (195.1 m^2/g), and large pore volume (0.53 cm^3/g). Different from previous reports in which block copolymer and surfactant are dual templates,[18] we utilized porous polymer microspheres as a template to form the hierarchical mesoporous silica microspheres. These microspheres are used as a new protein (BSA) adsorbent which shows high protein adsorption capacity (260 mg/g) and a fast adsorption rate (reaching equilibrium with 8 h)

EXPERIMENTAL SECTION

Materials. The silica precursor tetraethylorthosilane (TEOS) were purchased form Alfa Asear. The template polymer microspheres are a polymer of glycidyl methacrylate (GMA) cross-linked with ethylene glycol dimethacrylate (EGDMA) supplied by Nano-Micro Technology

Received: February 29, 2012
Accepted: April 27, 2012
Published: April 27, 2012

Scheme 1. Formation of Hierarchically Mesoporous Silica Microspheres Embedded with Magnetic Nanoparticles

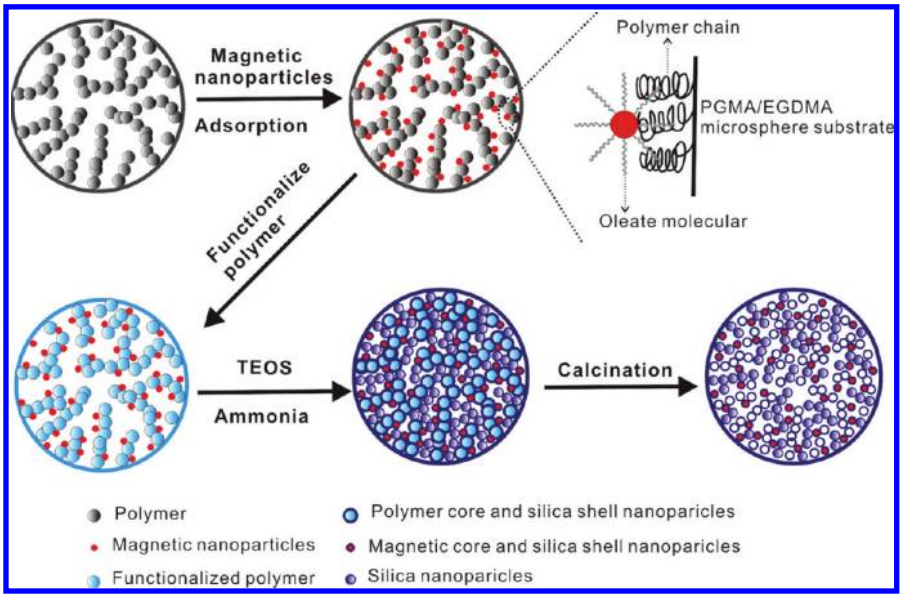

Company, China. Ferric chloride hexahydrate ($FeCl_3$ $6H_2O$), sodium oleate, trimethylamine (TMA) hydrochloride, sodium hydroxide, ammonium hydroxide (28% aqueous solution) and ethanol were purchased from Shanghai Chemical Reagent Corp, China. Hexanes, chloroform, and 1-octadecene were purchased from Alfa Aesar. Bovine serum albumin (BSA) was purchased from Sigma (St. Louis, MO, USA). Water was purified by distillation followed by deionization using ion exchange resins. Other chemicals were analytical grade and used without any further purification.

Synthesis of Magnetic γ-Fe_2O_3 Nanoparticles. Monodisperse magnetic γ-Fe_2O_3 nanoparticles were synthesized through the thermal decomposition of organometallic precursors with modifications.[19] Typically, 10 g of ferric chloride hexahydrate and 35 g of sodium oleate were dissolved in a mixture of 90 mL of ethanol, 70 mL of water, and 130 mL of hexane. The mixed solution was heated to 70 °C for 4 h. The resulting ferric oleate was washed four times with 50 mL of distilled water and dried at 50 °C. Thirty-six grams of the iron-oleate complex synthesized as described above and 5.7 g of oleic acid were dissolved in 200 g of 1-octadecene at room temperature. The reaction mixture was heated to 320 °C with a constant heating rate of 3.3 °C min^{-1}, and then kept at 320 °C for 30 min. When the reaction temperature reached 320 °C, the initial transparent solution became turbid and brownish black. The resulting solution containing the nanoparticles was then cooled to room temperature, and 500 mL of ethanol was added to the solution to precipitate the nanoparticles, which were subsequently separated by centrifugation. The weight of dry oleate-capped magnetic nanoparticles was 8.2 g.

Preparation of Magnetic Polymer Composite Microspheres Doped with γ-Fe_2O_3 Nanoparticles. 0.2 g magnetic nanoparticles were added in 50 mL of toluene. After ultrasonic treatment in water bath in 1 h, a homogeneous yellow solution was obtained. Another 100 mL of toluene containing 2 g of P(GMA-EGDMA) microspheres was prepared. Under stirring, the magnetic nanoparticles solution was added into the polymer microspheres solution. After 2 h, magnetic nanoparticles embedded porous polymer microspheres were filtrated and washed repeatedly with toluene and ethanol. The brown magnetic polymer composite microspheres were dried at 50 °C under vacuum.

Surface Modification Magnetic Polymer Composite Spheres. Two grams of brown composite spheres were dispersed in 250 mL of a mixture of ethanol and water (volume ratio = 2/1). And then, 2 g of trimethylamine hydrochloride and 1 g of sodium hydroxide were added to the mixture solution. After the result mixture was stirring in water bath at 50 °C for 24 h, the resulting TMA-treated magnetic P(GMA-EGDMA) composite microspheres were filtrated and washed repeated with distilled water. The brown functionalized magnetic polymer composite microspheres were dried at 50 °C under vacuum.

Preparation of Hierarchically Mesoporous Magnetic Silica Microspheres. In a 250-ml three-necked, rounded-bottomed flask equipped with a mechanical stirrer was placed 80 mL of ethanol and 20 g of water. With vigorous stirring in the flask, 0.5 g the TMA-treated magnetic P(GMA-EGDMA) composite microspheres and 2 mL of ammonia hydroxide were introduced over a period of 0.5 h. A 10% TEOS solution (in ethanol) of 30 mL was then added dropwise into the mixture in 1.5 h. The sol−gel transformation of TEOS to silica in the pore of the magnetic polymer microspheres was carried out at 30 °C for 24 h. The brown γ-Fe_2O_3/polymer/silica microspheres obtained were washed repeatedly with ethanol and distilled water before being dried at 50 °C overnight. The dried microspheres were calcinated at 600 °C for 10 h (ramp rate of 10 °C/min) under air. After calcination, the yellow hierarchical porous magnetic silica microspheres were obtained.

Protein Adsorption Experiment. Generally, BSA was dissolved in sodium phosphate buffer (20 mM) at pH 7.0 to make a stock solution (5.0 mg/mL). A mixture of 50 mL of 5.0 mg/mL protein solution and 100 mg of the material was shaken at 4 °C. At a given time, 0.5 mL of emulsion solution was extracted and then centrifuged at 15 000 rpm for 3 min, followed by the extraction of the upper clear solution for UV analysis at 280 nm.

Characterizations. The morphology and structure of the magnetic polymer microspheres were studied using a field emission scanning electron microscope (Hitach S4800) and a transmission electron microscope (FEI Tecnai G2). The particle hydrodynamic size was measured by using a Beckman Coulter Counter laser size analyzer (Multisizer 3). The infrared spectra were recorded using potassium bromide on a Shimadzu IR Prestige-21 and the thermogravimetric analysis was conducted on a Du Pont TGA 2050, with a temperature ramp of 10 °C min^{-1}. The magnetization curve was measured at room temperature under a varying magnetic field with a varying magnetic field with vibrating sample magnetometer (ISOM, UPM, Madrid). N2 adsorption and desorption isotherms were measured at 77K on a Micromeritics tristar II 3020. The XRD pattern of prepared powder sample was collected using a Rigaku D/Max-2200PC X-ray diffractometer with Cu targer (40KV, 40 mA). The γ-Fe_2O_3 content in the silica microspheres was determined by atomic absorption spectroscopy (AAS, Perkin-Elmer 3110) of an extract from the sample obtained with dilute HCl (1:1) and HF (1:1) at 80 °C for 6 h. UV absorbance spectra measured using a NanoDrop 2000 Spectrophotometer (Thermo Fisher Scientific, USA).

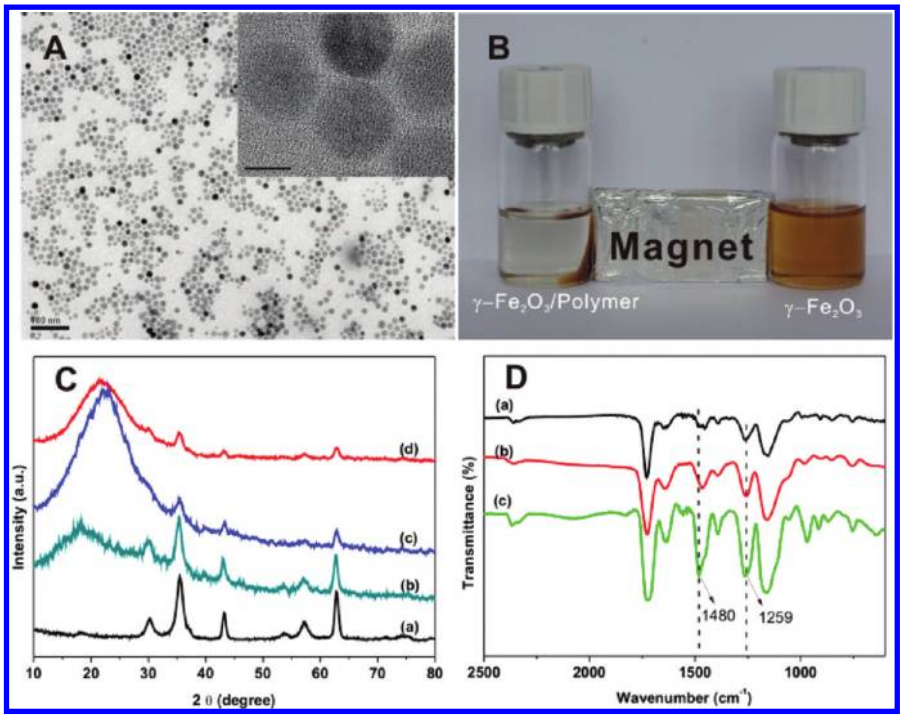

Figure 1. (A) TEM image of the monodisperse magnetic nanoparticle. (B) Photograph of magnetic nanoparticles (right) and magnetic nanoparticles embedded in polymer microspheres (left) separation from toluene after adding an external magnetic field in 1 min. (C) XRD pattern of (a) γ-Fe_2O_3, (b) γ-Fe_2O_3/polymer, (c) γ-Fe_2O_3/polymer/SiO_2, and (d) γ-Fe_2O_3/SiO_2. (D) FT-IR spectrum of (a) polymer, (b) γ-Fe_2O_3/polymer, and (c) functionalized γ-Fe_2O_3/polymer.

RESULTS AND DISCUSSION

A schematic synthesis procedure is shown in Scheme 1. The monodisperse porous microspheres used as template are a commercial available polymer of glycidyl methacrylate (GMA) cross-linked with ethylene glycol dimethacrylate (EGDMA) with designed pore size and narrow size distribution. The porous P(GMA/EGDMA) microspheres were well dispersed in toluene. First, monodisperse γ-Fe_2O_3 nanoparticles stabilized with hydrophobic oleic acid ligand were transferred into a channel of porous polymer microspheres through strong hydrophobic interactions between the P(GMA/EGDMA) polymer chain and the magnetic nanoparticles capping agents in toluene, producing porous polymer microspheres doped with magnetic nanoparticles. Second, the porous P(GMA/EGDMA) microspheres were functionalized with a quaternary amine group via ring-opening reaction of epoxide groups of GMA with trimethylamine (TMA). Third, the silica nanoparticles were deposited into a channel of functionalized porous magnetic polymer microspheres through sol–gel reaction with tetraethylorthosilane (TEOS), resulting in uniform magnetic polymer/silica composite microspheres. Finally, hierarchically mesoporous silica microspheres embedded with magnetic nanoparticles were obtained after calcinations to remove polymer template and organic agents.

Figure 1A shows transmission electron microscopy (TEM) images of monodisperse (~12 nm in diameters) magnetic nanoparticles. XRD pattern confirmed that the magnetic particles are γ-Fe_2O_3 nanoparticle.[20] With the oleic acid ligand capped on the surface, the magnetic nanoparticles could be well dispersed in toluene and stabilized for several months without precipitation. The content of γ-Fe_2O_3 in the oleate capped magnetic nanoparticles was 80.4%, which was determined by AAS. To conduct sol–gel reaction to form magnetic silica composite, it is necessary to transfer these hydrophobic ligand-capped nanoparticles from organic phase to aqueous phase.[21] Inspired by a recent report by Nie et al. on the "mesoscopic" pores of polymer microspheres and the hydrophobic interactions between the pore walls and the nanoparticle capping agents,[22] we used the matrix of porous P(GMA/EGDMA) microsphere to support the magnetic nanoparticles. The scanning electron microscopy (SEM) images of the polymer microspheres are shown in Figure 2A–C.

The monodisperse polymer microspheres are 3.4 μm in diameter having a porous outer surface and a porous inner surface. The pore size is around 70 nm with Brunauer–Emmett–Teller (BET) = 40.5 m^2/g, pore volume = 0.29 cm^3/g. The intrinsic hydrophobic nature of porous P(GMA/EGDMA) microspheres is well suited for incorporating oleic acid coated magnetic nanoparticles, which move into the pore by diffusion and are trapped by strong hydrophobic interactions. This partitioning process was so rapid and quantitative that essentially no magnetic nanoparticles were left in toluene after one hour. We used the laser size analyzer to investigate the diameter change of the polymer microsphere in this process. We found that the diameter of such a polymer microsphere incorporated with magnetic nanoparticles was similar to that of template microsphere (Figure 2J), which indicates that the polymer microsphere did not swell and magnetic nanoparticles could not swell in the polymeric phase of template microspheres in toluene. The dispersed magnetic nanoparticles embedded in the polymer microspheres is a light brown solution. When applied an external magnetic field, the magnetic nanoparticles incorporated polymer microspheres could be attracted in 1 min by the magnet. In contrast, magnetic nanoparticle dispersion solution was not affected by the magnet because the capped agent stabilizes such nanoparticles in toluene (Figure 1B). The size and dispersion

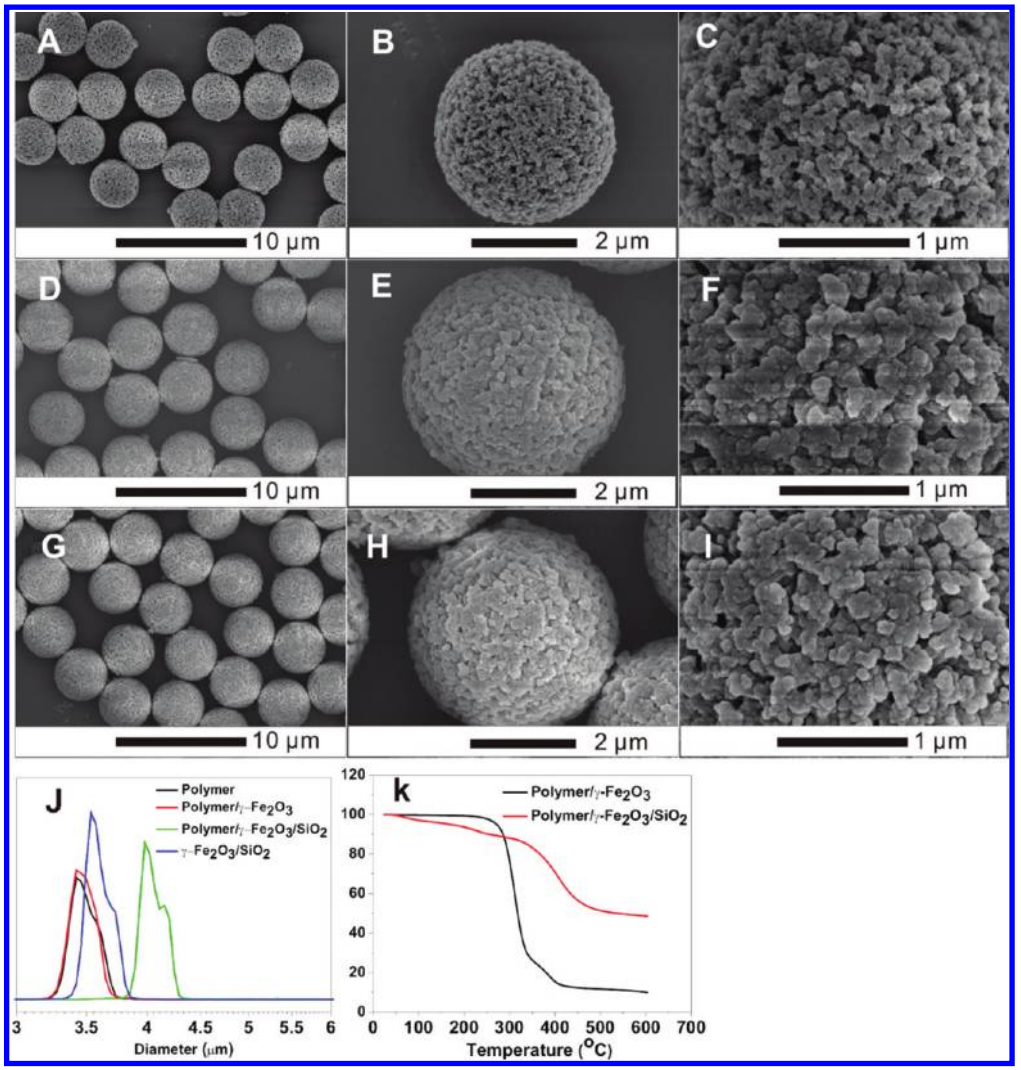

Figure 2. SEM images of (A–C) polymer microspheres, (D–F) γ-Fe_2O_3/polymer/SiO_2 microspheres and (G–I) γ-Fe_2O_3 /SiO_2 microspheres. (J) The particle size distribution of polymer, polymer/γ-Fe_2O_3, polymer/γ-Fe_2O_3/SiO_2 and γ-Fe_2O_3/SiO_2 microspheres. (K) TGA curve of polymer/γ-Fe_2O_3/ SiO_2 and γ-Fe_2O_3/ SiO_2 microspheres.

property of such composites microspheres are the same as the undoped polymer microspheres, suggesting the incorporating process of magnetic nanoparticles does not destroy the polymer matrix (Figure 2K). Figure 1C shows the X-ray diffraction (XRD) patterns of the composites microspheres exhibit diffraction patterns similar to that of γ-Fe_2O_3 nanoparticles. The board XRD reflection peak at $2\theta = 22°$ can be assigned to the diffraction of amorphous structures of the polymer microsphere hosts.

Although the magnetic nanoparticles were incorporated into the porous polymer matrix by the strong hydrophobic interactions, two major concerns in biological detection with microspheres as carriers remain: first is the leakage of hydrophobic nanoparticles dissolving into background solution; and second is the weakly hydrophilic property of matrix microspheres.[23] To prevent the leakage of magnetic nanoparticles and improve the biocompatibility of the polymer microspheres, we chose silica for the coating of magnetic polymer microspheres. In our hands, the porous magnetic P(GMA/EGDMA) microspheres were functionalized by ring-opening reaction of epoxy group with TMA, leading to the formation of quaternary amine on the polymer surface. It was reported that the modified polymer microsphere which was functionalized with $-NH_2$ group could be coated with uniform silica shells using a modified Stober method.[24] To characterize the structure change of polymer, FT-IR spectrum was recorded, shown in figure 1D. The FT-IR spectra of the functionalized magnetic polymer microspheres were similar to that of the original polymer microspheres, with a slight shift of wave numbers. The most difference between these spectra was the appearance of the new peaks at 1480 cm^{-1}, which was assigned to methyl groups of ammonium.[25] The functionalization process of the polymer did not induce the doped magnetic nanoparticles to leak from the matrix of the microspheres because the hydrophobic polymer chain and the pore structure of the PGMA/EGDMA microspheres were reserved during the reaction.

Figure 2D–F shows the SEM images of silica coated on the template microspheres after sol–gel reaction. The hybrid microspheres are mostly monodisperse with negligible aggregation. The diameter of the hybrid microsphere is about 4.0 μm which is larger than the template microspheres, indicating successful coating of magnetic polymer microsphere with silica. At high magnification, open pores of various sizes

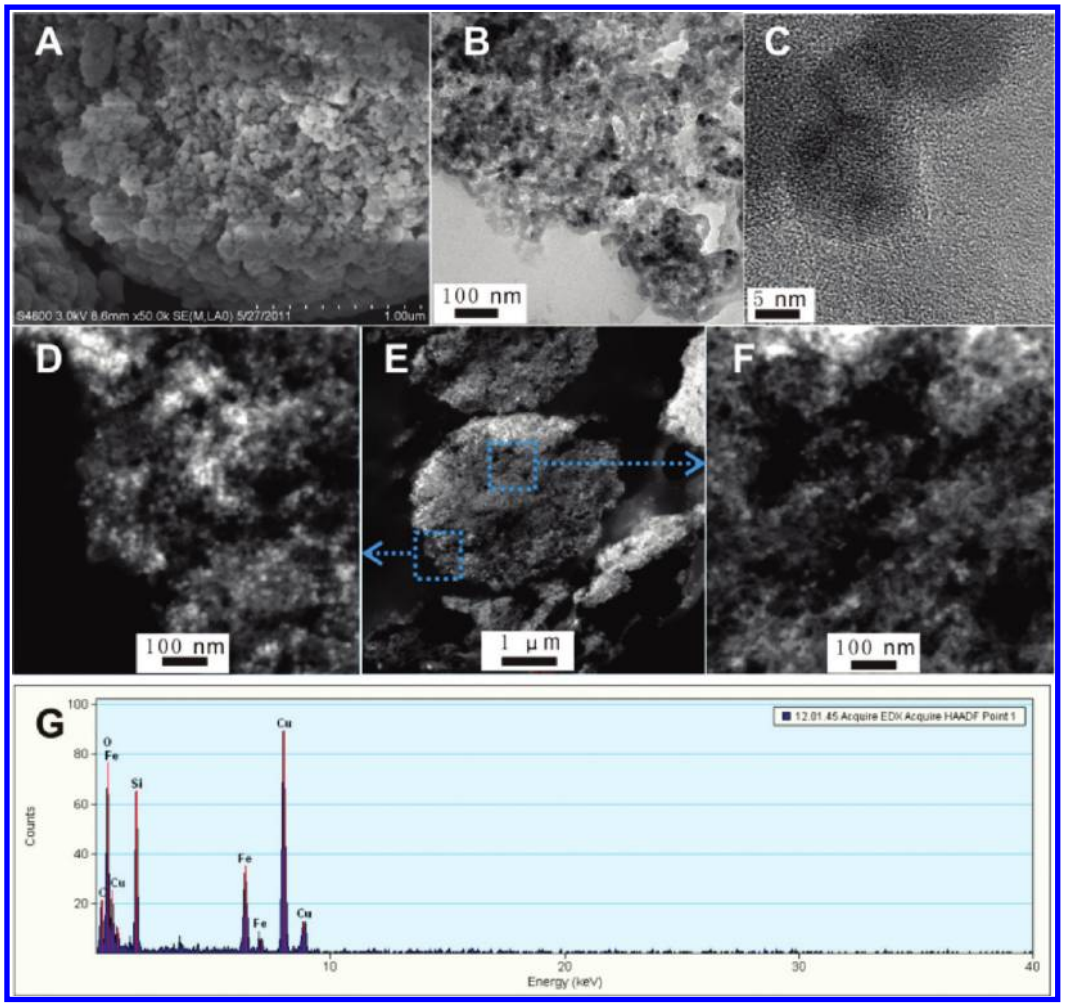

Figure 3. (A) SEM image of the inner structure of γ-Fe_2O_3/SiO_2 microspheres. (B−C) TEM image of the crashed γ-Fe_2O_3/ SiO_2 microspheres. (D−F) STEM images of γ-Fe_2O_3/SiO_2 microspheres. (G) EDX map γ-Fe_2O_3/SiO_2 microspheres.

and aggregates of fine particles about 30 nm were observed on the surface, different from template microspheres. The electrostatic interaction between the positively charged magnetic polymer surface and the hydrolyzed negatively charged silica moieties is tentatively considered to be the driving force for the successful deposition. The subsequent calcination at 600 °C produced porous magnetic silica microspheres. Thermogravimetric analysis (TGA) was used to study the silica component of the magnetic polymer/silica microspheres, and the results are shown in Figure 2K. The weight loss up to 600 °C was calculated to be 90.1 wt % and 48.5 wt % for the γ-Fe_2O_3/polymer template microspheres and their silica hybrid microspheres, respectively. The weight loss in this temperature range is mostly attributed to the degradation of polymer chains of microspheres and organic agent of oleate capped magnetic nanoparticles. The difference of weight loss ratio of two samples indicated that the silica was successfully deposited on the template microspheres and the content of silica in the magnetic polymer/silica microspheres was calculated to be about 40%. The SEM images (Figure 2G−I) demonstrate that the resulting materials are monodisperse porous microspheres and the surface morphology of the silica microspheres is similar to that of the γ-Fe_2O_3/polymer/silica hybrid microspheres. The diameter of γ-Fe_2O_3/silica microspheres is about 3.5 μm, which is much smaller than the size of the γ-Fe_2O_3/polymer/silica microspheres before calcination but closer to the size of γ-Fe_2O_3/polymer template microspheres. The particle hydrodynamic size analyzer (Figure 2J) shows that the determined particle sizes are close to those measured by SEM.

The details of the internal structure of the γ-Fe_2O_3/silica microspheres are shown in Figure 3A−F. SEM image (Figure 3A) of a broken γ-Fe_2O_3/silica microspheres shows that the morphology inside the microsphere is similar to that on the surface, and the pores are open with connecting channels. Furthermore, fine silica particles of about 30 nm are discernible. TEM (Figure 3B,C) are used to probe the cross-section view of the γ-Fe_2O_3/silica microspheres which exhibit a random, interconnected internal pore structure with mesopores in the range of 10−100 nm. Uniform nanoparticles (~10 nm) were found to be encapsulated in the matrix of porous silica. Scanning transmission electron microscopy (STEM) was used to characterize the dispersity of nanoparticles in the matrix of porous silica microspheres. As shown in figure 3 (D-F), monodisperse nanoparticles (the bright spots in the STEM image) are well-dispersed in the whole range of porous silica microspheres besides the edge area (Figure 3D) and central area (Figure 3F). Energy-dispersive X-ray (EDX) analysis of the bright-spot area in figure 3D clearly showed the presence of Fe (γ-Fe_2O_3) and Si (SiO_2). An XRD pattern of the composite microspheres is shown in figure 1C, the characteristic diffraction peaks of γ-Fe_2O_3 are observed, which is consistent

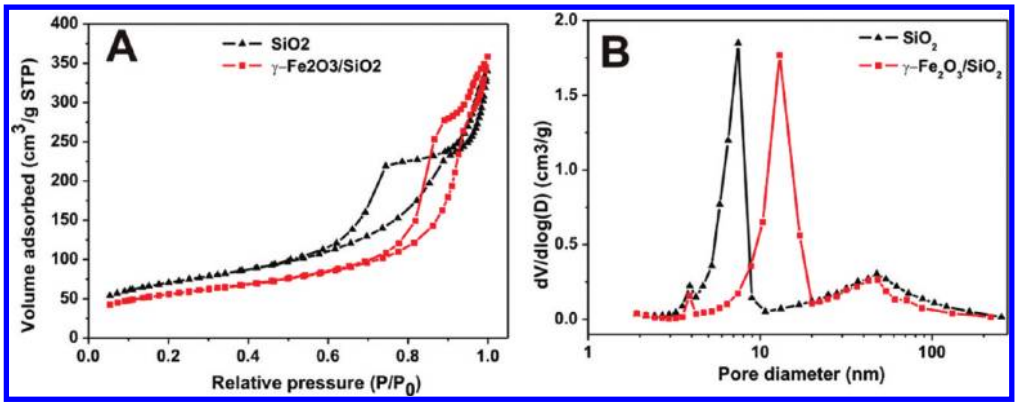

Figure 4. N_2 adsorption/desorption isotherms and pore size distributions of sample SiO_2 and γ-Fe_2O_3/SiO_2 microspheres.

Table 1. Properties of Template and Different Type of Synthesized Microspheres

microsphere materials	particle size (mean + SD) μm	BET surface area (m^2 g^{-1})	pore volume (cm^3 g^{-1})	pore size distribution (nm)		
P(GMA/EGDMA)	3.42 ± 0.173	40.5	0.29		70	
Fe_2O_3/polymer/SiO_2	3.97 ± 0.184	23.5	0.18		50	
Fe_2O_3/SiO_2	3.53 ± 0.156	195.1	0.53	3.8	13.2	47.5
SiO_2	3.48 ± 0.161	244.3	0.51	3.8	7.4	48.2

with EDX results and further confirms the existence of magnetic nanoparticles in the porous silica microspheres. The γ-Fe_2O_3 nanoparticles content was 8.1% in the magnetic silica microspheres which was determined by AAS.

To confirm the existence of hierarchically mesoporous structure in the resulting microspheres, we investigated the N_2 adsorption/desorption isotherms and pore size distributions of the porous γ-Fe_2O_3/silica microspheres. Figure 4 shows a type IV isotherm with two major capillary condensation steps at relative pressure P/P_0 ranges 0.8−0.9 and 0.9−1.0, which is a characteristic of hierarchical porous architectures. The pore size distribution curve shows that the primary, secondary and tertiary pore diameters are centered at 3.8 nm, 13.2 and 44.7 nm respectively, indicating that the materials have unique hierarchical porous structures on at least three levels. The BET surface area and pore volume are 195.1 m^2/g and 0.53 cm^3/g, respectively. The majority of the available surface area is due to the presence of the mesopore at 13.2 nm, which means that during the porous polymer matrix template extraction process by calcination the samples shrink. The smaller pore at 3.8 nm might be formatted from the functionalized polymer chain because of the TEOS molecules could permeate the surface of the polymer template.[26,27] Furthermore, the larger mesopore at 44.7 nm is the size of interparticles between the silica nanoparticles. To further demonstrate the mechanism of hierarchical mesopore formation, we also synthesized the porous silica microspheres in absence of magnetic nanoparticle under the similar conditions. The morphology of the result microspheres is similar to the γ-Fe_2O_3/silica microspheres. There are also the existence of three pore structures from the N_2 adsorption/desorption isotherms and pore size distributions analysis (Table 1). Interestingly, the small and lager mesopores did not change much but the second mesopore changed from 13.2 to 7.4 nm, suggesting that the oleic acid ligand-capped magnetic nanoparticle participated in the formation of the main mesopore structure. Because of the magnetic nanoparticles adsorbed inside the channel of the porous polymer microspheres and silica coated on the surface of hybrid microspheres matrix in the sol−gel reaction, the main mesopore at 13.4 nm should be formed from the polymer matrix shrinkage and oleic acid ligands extraction under the calcination process.

The magnetic properties were investigated with a vibrating sample magnetometer at 300 K, as shown in magnetization curves in Figure 5. The γ-Fe_2O_3 nanoparticles, polymer/γ-Fe_2O_3 microspheres, polymer/γ-Fe_2O_3/SiO_2 microspheres, and γ-Fe_2O_3/SiO_2 microspheres have saturation magnetization values of 15.5, 8.1, 4.3, and 8.2 emu/g, respectively. The polymer/γ-Fe_2O_3 and γ-Fe_2O_3/SiO_2 microspheres have similar saturation magnetization values which indicate that the γ-Fe_2O_3 content in these microspheres is similar. This experimental result is consistent with the TGA result of polymer/γ-Fe_2O_3/SiO_2 microspheres, in which the silica and polymer content is calculated to be about 40%, respectively, in the polymer/γ-Fe_2O_3/SiO_2 microspheres. The magnetic porous γ-Fe_2O_3/SiO_2 microspheres could be well-dispersed in water to form a transparent yellow solution. The porous microspheres in their homogeneous dispersion show fast movement to the applied magnetic field and could be attracted to the side wall of vial

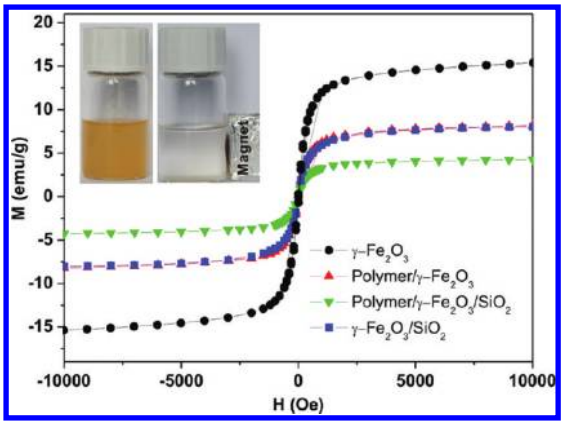

Figure 5. Magnetic hysteresis curves of γ-Fe_2O_3, γ-Fe_2O_3/polymer, γ-Fe_2O_3/polymer/SiO_2, and γ-Fe_2O_3/SiO_2 microspheres. The inset is a photograph of γ-Fe_2O_3/SiO_2 microspheres under external magnetic field.

completely by magnet within 1 min (Figure 5 inset). This excellent magnetic responsivity and redispersibility may be a useful property in the field of immobilization and magnetic separation of biomoleculars.

Mesoporous materials with novel pore properties are preferable adsorbents for biomaterial immobilization.[28−31] Many efforts have been made in this research area. Encouraged by the hierarchically porous structure and magnetic properties of the microspheres, we have explored the potential applications of our new materials in immobilization and magnetic separation of protein. BSA was used as a model protein. BSA is a large biomolecule with molecular weight of 66.4 kDa and dimensions of 5.0 × 7.0 × 7.0 nm. BSA adsorption kinetics with sodium phosphate buffer (20 mM) at pH 7.0 for 20 h with an initial BSA concentration of 5 mg/mL is shown in Figure 6. The adsorption capacity was 260 mg/g

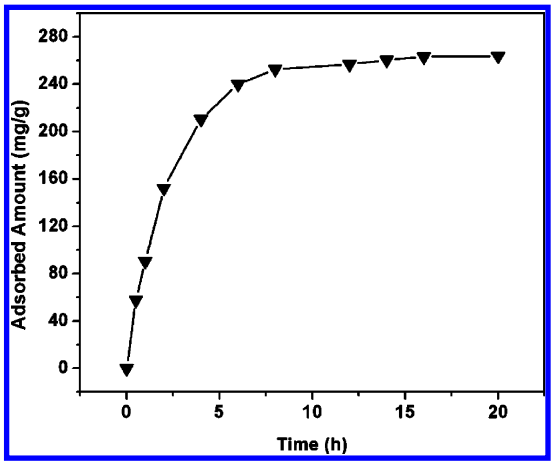

Figure 6. BSA adsorption kinetics on hierarchically mesoporous magnetic silica microspheres.

which is higher than MCM-41 with a monomodel small pore diameter.[32] Meanwhile, the adsorption rate was fast. The adsorption saturation of BSA was reached in 8 h for the hierarchically porous microspheres (see Table 2), which is faster than that of SBA-15 with the equilibrium time of 24 h.[33] The high content of pores is a key factor that influences adsorption rate and capacity. The SEM images show that there was a high content of large pores on the surface, so protein molecules entered the interior of spheres with less resistance. Besides, large amount of mesopore inside the microspheres ensure the fast and abundant adsorption of proteins. Furthermore, an important advantage of employing such magnetic porous microspheres to immobilize biomolecules is that they can be easily recovered from the reaction media by means of an external magnetic field.

CONCLUSIONS

We have prepared magnetic porous polymer microspheres by incorporating monodisperse iron oxide nanoparticle into the porous polymer microspheres. By employing a functionalized magnetic polymer microspheres template in the sol−gel process, previously unattainable micrometer-sized porous silica microspheres embedded with the magnetic nanoparticle can now be easily prepared in high yields. The microspheres possess uniform particle size, hierarchically mesoporous structure, high surface area, large pore volume and high magnetization. The products have shown a high protein adsorption capacity (260 mg/g) and fast adsorption rate (8 h) to BSA, demonstrating great potential in biomacromolecular magnetic separation. In addition, the approach demonstrated in this work may allow synthesis of nanoparticles or semiconductor quantum dots (e.g., CdSe, Au) embedded in hierarchical mesoporous silica microspheres with potential applications in enzyme immobilization, catalyst, and analytical detection.

AUTHOR INFORMATION

Corresponding Author

*E-mail: jiangbw@pkusz.edu.cn (B.J.); jingzhao@nju.edu.cn (J.Z.).

Notes

The authors declare no competing financial interest.

ACKNOWLEDGMENTS

This work was financially supported by the Shenzhen-Hong Kong Innovative Circle Project, China (ZYB200907080082A). This work is financially supported by grants of National Basic Research Program of China (2010CB923303 to J.Z.). J.Z. thanks National Natural Science Foundation of China (91013009) for support. Project supported by the Fok Ying-Tong Education Foundation, China (132011 to J.Z.).

REFERENCES

(1) Zhang, L.; Qiao, S.; Jin, Y.; Yang, H.; Budihartono, S.; Stahr, F.; Yan, Z.; Wang, X.; Hao, Z.; Lu, G. Q. *Adv. Funct. Mater.* **2008**, *18*, 3203−3212.

(2) Deng, Y.; Cai, Y.; Sun, Z.; Liu, J.; Liu, C.; Wei, J.; Li, W.; Liu, C.; Wang, Y.; Zhao, D. *J. Am. Chem. Soc.* **2010**, *132*, 8466−8473.

(3) Valdes-Solis, T.; Rebolledo, A. F.; Sevilla, M.; Valle-Vigon, P.; Bomati-Miguel, O.; Fuertes, A. B.; Tartaj, P. *Chem. Mater.* **2009**, *21*, 1806−1814.

(4) Ruiz-Hernandez, E.; Lopez-Noriega, A.; Arcos, D.; Izquierdo-Barba, I.; Terasaki, O.; Vallet-Regi, M. *Chem. Mater.* **2007**, *19*, 3455−3463.

(5) Wang, P.; Shi, Q.; Shi, Y.; Clark, K. K.; Stucky, G. D.; Keller, A. A. *J. Am. Chem. Soc.* **2009**, *131*, 182−188.

(6) Wang, C.; Tao, S.; Wei, W.; Meng, C.; Liu, F.; Han, M. *J. Mater. Chem.* **2010**, *20*, 4635−4641.

(7) Deng, Y.; Qi, D.; Deng, C.; Zhang, X.; Zhao, D. *J. Am. Chem. Soc.* **2008**, *130*, 28−29.

(8) Guo, X.; Deng, Y.; Gu, D.; Che, R.; Zhao, D. *J. Mater. Chem.* **2009**, *19*, 6706−6712.

(9) Gai, S.; Yang, P.; Li, C.; Wang, W.; Dai, Y.; Niu, N.; Lin, J. *Adv. Funct. Mater.* **2010**, *20*, 1166−1172.

Table 2. Adsorption Results of BSA on Different Mesoporous Silica Sphere Materials

type	BSA adsorption (mg/g)	time (h)	particle size (μm)	BET surface area (m^2 g^{-1})	pore volume cm^3 g^{-1}	pore size distribution (nm)		
MCM-41	150	24	nanometer	890	0.79		1.88	
SBA-15	20	20	4−10	768	1.63		12.7	
Our product	260	8	3.48	195	0.51	3.8	13.2	47.5

(10) Piaoping, Y.; Zewei, Q.; Zhiyao, H.; Chunxia, L.; Xiaojiao, K.; Ziyong, C.; Jun, L. *Biomaterials* **2009**, *30*, 4786−4795.
(11) Zhao, W.; Chen, H.; Li, Y.; Li, L.; Lang, M.; Shi, J. *Adv. Funct. Mater.* **2008**, *18*, 2780−2788.
(12) Li, L.; Choo, E. S. G.; Tang, X.; Ding, J.; Xue, J. *Chem. Commun.* **2009**, 938−940.
(13) Zhang, L.; Qiao, S.; Jin, Y.; Chen, Z.; Gu, H.; Lu, G. Q. *Adv. Mater.* **2008**, *20*, 805−806.
(14) Kim, J.; Lee, J. E.; Lee, J.; Yu, J. H.; Kim, B. C.; An, K.; Hwang, Y.; Shin, C. H.; Park, J. G.; Hyeon, T. *J. Am. Chem. Soc.* **2006**, *128*, 688−689.
(15) Kim, J.; Kim, H. S.; Lee, N.; Kim, T.; Kim, H.; Yu, T.; Song, I. C.; Moon, W. K.; Hyeon, T. *Angew. Chem., Int. Ed.* **2008**, *47*, 8438−8441.
(16) Liong, M.; Lu, J.; Kovochich, M.; Xia, T.; Ruehm, S. G.; Nel, A. E.; Tamanoi, F.; Zink, J. I. *Acs Nano* **2008**, *2*, 889−896.
(17) Lin, Y.-S.; Haynes, C. L. *Chem. Mater.* **2009**, *21*, 3979−3986.
(18) Niu, D.; Ma, Z.; Li, Y.; Shi, J. *J. Am. Chem. Soc.* **2010**, *132*, 15144−15147.
(19) Park, J.; An, K. J.; Hwang, Y. S.; Park, J. G.; Noh, H. J.; Kim, J. Y.; Park, J. H.; Hwang, N. M.; Hyeon, T. *Nat. Mater.* **2004**, *3*, 891−895.
(20) Hyeon, T.; Lee, S. S.; Park, J.; Chung, Y.; Bin Na, H. *J. Am. Chem. Soc.* **2001**, *123*, 12798−12801.
(21) Lei, Z.; Shi Zhang, Q.; Lina, C.; Zifeng, Y.; Gao Qing, L. *Nanotechnology* **2008**, *19*, 435608.
(22) Sathe, T. R.; Agrawal, A.; Nie, S. *Anal. Chem.* **2006**, *78*, 5627−5632.
(23) Li, Y.-H.; Song, T.; Liu, J.-Q.; Zhu, S.-J.; Chang, J. *J. Mater. Chem.* **2011**, *21*, 12520−12528.
(24) Lu, Y.; McLellan, J.; Xia, Y. N. *Langmuir* **2004**, *20*, 3464−3470.
(25) Qin, C. Q.; Xiao, Q.; Li, H. R.; Fang, M.; Liu, Y.; Chen, X. Y.; Li, Q. *Int. J. Biol. Macromol.* **2004**, *34*, 121−126.
(26) Su, Y.; Yan, R.; Dan, M.; Xu, J.; Wang, D.; Zhang, W.; Liu, S. *Langmuir* **2011**, *27*, 8983−8989.
(27) Wang, S.; Zhang, M.; Wang, D.; Zhang, W.; Liu, S. *Microporous Mesoporous Mater.* **2011**, *139*, 1−7.
(28) Jaeyun, K.; Yuonzhe, P.; Nohyun, L.; Yong ll, P.; In-Hwon, L.; Jung-Ho, L.; Paik, S. R.; Toeghwon, H. *Adv. Mater.* **2010**, *22*, 57−60.
(29) Chen, L.; Zhu, G.; Zhang, D.; Zhao, H.; Guo, M.; Shi, W.; Qiu, S. *J. Mater. Chem.* **2009**, *19*, 2013−2017.
(30) Sun, Z.; Deng, Y.; Wei, J.; Gu, D.; Tu, B.; Zhao, D. *Chem. Mater.* **2011**, *23*, 2176−2184.
(31) Valdes-Solis, T.; Rebolledo, A. F.; Sevilla, M.; Valle-Vigon, P.; Bomati-Miguel, O.; Fuertes, A. B.; Tartaj, P. *Chem. Mater.* **2009**, *21*, 1806−1814.
(32) Katiyar, A.; Ji, L.; Smirniotis, P. G.; Pinto, N. G. *Microporous Mesoporous Mater.* **2005**, *80*, 311−320.
(33) Katiyar, A.; Yadav, S.; Smirniotis, P. G.; Pinto, N. G. *J. Chromatogr. A* **2006**, *1122*, 13−20.